

# Weak value amplified optical activity measurements

Marcel Pfeifer\* and Peer Fischer

Fraunhofer Institute for Physical Measurement Techniques,  
79110 Freiburg, Germany

[\\*marcel.pfeifer@ipm.fraunhofer.de](mailto:marcel.pfeifer@ipm.fraunhofer.de)

**Abstract:** We present a new form of optical activity measurement based on a modified weak value amplification scheme. It has recently been shown experimentally that the left- and right-circular polarization components refract with slightly different angles of refraction at a chiral interface causing a linearly polarized light beam to split into two. By introducing a polarization modulation that does not give rise to a change in the optical rotation it is possible to differentiate between the two circular polarization components even after post-selection with a linear polarizer. We show that such a modified weak value amplification measurement permits the sign of the splitting and thus the handedness of the optically active medium to be determined. Angular beam separations of  $\Delta\theta \sim 1$  nanoradian, which corresponds to a circular birefringence of  $\Delta n \sim 1 \times 10^{-9}$ , could be measured with a relative error of less than 1%.

© 2011 Optical Society of America

**OCIS codes:** (120.0120) Instrumentation, measurement, and metrology; (120.5710) Refraction; (160.1585) Chiral media; (260.1440) Birefringence.

---

## References and links

1. Y. Aharonov, D. Z. Albert, and L. Vaidman, "How the result of a measurement of a component of the spin of a spin-1/2 particle can turn out to be 100," *Phys. Rev. Lett.* **60**, 1351–1354 (1988).
2. I. M. Duck, P. M. Stevenson, and E. C. G. Sudarshan, "The sense in which a 'weak measurement' of a spin-1/2 particle's spin component yields a value 100," *Phys. Rev. D* **40**, 2112–2117 (1989).
3. N. W. M. Ritchie, J. G. Story, and R. G. Hulet, "Realization of a measurement of a 'weak value'," *Phys. Rev. Lett.* **66**, 1107–1110 (1990).
4. O. Hosten and P. Kwiat, "Observation of the spin hall effect of light via weak measurements," *Science* **319**, 787–790 (2008).
5. P. B. Dixon, D. J. Starling, A. N. Jordan, and J. C. Horwell, "Ultrasensitive beam deflection measurement via interferometric weak value amplification," *Phys. Rev. Lett.* **102**, 173601 (2009).
6. L. D. Barron, *Molecular Light Scattering and Optical Activity*, 2nd ed. (Cambridge University Press, 2004).
7. A. Fresnel, *Œuvres complètes d'Augustin Fresnel*, H. d. Sénarmont, E. Verdet, and L. Fresnel, eds. (Imprimerie impériale, Paris, 1866), Vol. 1.
8. A. Ghosh and P. Fischer, "Chiral molecules split light: reflection and refraction in a chiral liquid," *Phys. Rev. Lett.* **97**, 173002 (2006).
9. A. Ghosh, F. M. Fazal, and P. Fischer, "Circular differential double diffraction in chiral media," *Opt. Lett.* **32**, 1836–1838 (2007).
10. M. P. Silverman, "Reflection and refraction at the surface of a chiral medium: comparison of gyrotropic constitutive relations invariant or noninvariant under a duality transformation," *J. Opt. Soc. Am. A* **3**, 830–837 (1986).
11. M. P. Silverman and J. Badoz, "Interferometric enhancement of chiral asymmetries: ellipsometry with an optically active Fabry-Perot interferometer," *J. Opt. Soc. Am. A* **11**, 1894–1917 (1994).
12. I. J. Lalov and E. M. Georgieva, "Multibeam interference, total internal reflection and optical activity," *J. Mod. Opt.* **44**, 265–278 (1997).
13. A. Ghosh, W. Hill, and P. Fischer, "Observation of the Faraday effect via beam deflection in a longitudinal magnetic field," *Phys. Rev. A* **76**, 055402 (2007).

14. A. Aiello, and J. P. Woerdman, "Role of beam propagation in Goos-Hänchen and Imbert-Fedorov shifts," *Opt. Lett.* **33**, 1437–1439 (2008).
15. J. C. Horwell, D. J. Starling, P. B. Dixon, P. K. Vudyasethu, and A. N. Jordan, "Interferometric weak value deflections: quantum and classical treatments," *Phys. Rev. A* **81**, 033813 (2010).
16. A. J. Leggett, "Comment on 'How the result of a measurement of a component of the spin of a spin-1/2 particle can turn out to be 100'," *Phys. Rev. Lett.* **62**, 2325 (1989).

## 1. Introduction

Ideally a measurement yields distinct (eigen)values that can be recorded by a suitable measuring device. Aharonov, Albert, and Vaidman (AAV) considered the case of "weak measurements" in quantum mechanics, where the measurement is unable to distinguish between (eigen)values after a weak perturbation [1, 2]. AAV showed that if prior to the measurement the system is prepared in a well-defined state, then a suitable post-selection can give rise to arbitrarily large expectation values and thereby permit the (eigen)values to be distinguished. They considered the displacement of the spin-components of a Gaussian ensemble of spin- $\frac{1}{2}$  particles that are detected on a screen after passing through two orthogonal Stern-Gerlach magnets. An optical weak value measurement was performed by Ritchie et al. [3], who showed that by carefully pre- and post-selecting the polarization state of a light beam, a weak value amplification scheme can be used to detect a lateral beam shift of  $0.64\ \mu\text{m}$  between the two linear-polarization components induced by a birefringent crystal. Hosten and Kwiat [4] reported the observation of an optical analog of the Spin Hall effect, where the lateral displacement of the two orthogonal linearly-polarized components of a light beam was measured via weak value amplification with  $\sim \text{\AA}$  sensitivity. Dixon et al. [5] similarly showed that beam deflections down to  $0.4\ \text{prad}$  could be detected in a Sagnac interferometer.

Here, we discuss how weak value amplification can be adapted to measure optical activity. The hallmark of natural and magnetic optical activity is that the medium has different refractive indices for right- and left- circularly polarized light, which causes the rotation of the plane of polarization of a linearly polarized light beam traversing the optically active medium. The small difference in refractive indices typically found in optically active systems can be detected in transmission (polarimetry) [6]. However, as Fresnel first proposed, it may also be detected in refraction [7]. A linearly polarized light beam incident at an interface between a chiral and an achiral medium will split into its two circular polarization components, as the two components refract with different angles of refraction [7, 8]. A position sensitive detector may be used to register the difference in beam positions [8, 9]. Optical activity measurements at interfaces require potentially much smaller fluid volumes than transmission experiments [8–13]. The sensitivity of the refraction scheme [7–9] depends on how small a separation between the left- and right-circular components can be registered on a detector. For chemical and pharmaceutical applications it is of interest to measure small optical activities (with correspondingly small refractive index differences) in minute liquid samples. Whilst weak value amplification has been used to determine small lateral beam shifts, we show that a conventional weak value measurement, as reported in the literature, does not provide sufficient information to determine the handedness of a chiral liquid. We have combined an appropriate polarization modulation scheme with a weak value measurement so that the handedness (sign) of weakly optically active media can be measured whilst still benefitting of an increase of up to  $10^6$  in the beam separation compared with the actual separation (in the absence of weak value amplification).

## 2. Theory

### 2.1. Weak measurements of small beam deflections

Weak measurements in optics that are based on polarization entail three steps: (1) preparation of the system in a defined (polarization) state, which is termed *pre-selection*, (2) a *weak interaction* giving rise to a (small) polarization-dependent beam deflection, and finally (3) *post-selection* of the final (polarization) state, which is chosen to be nearly orthogonal to the initial state. We now consider the case where the weak interaction is due to optical activity. A coherent light beam with a Gaussian beam profile is linearly polarized and is taken to be incident upon an optically active wedge (see Fig. 1). The wedge's optical activity can be natural, e.g. a chiral liquid in a triangular cuvette, or magnetic, e.g. due to a static magnetic field that is parallel to the light beam's direction of propagation (Faraday effect). The linear polarization state of the light is equivalent to a superposition of two circular polarization states (left- and right-circular) and these experience different refractive indices in the wedge. It follows that the two circular components refract with different angles of refraction at the second interface such that the light beam splits into two [8]. The handedness of the optically active medium determines which of the two circular components has the larger refractive index and hence the larger angle of refraction. This information is therefore crucial in natural optical activity measurements. In what follows we first describe how 'conventional' weak measurements can be used to detect minute angular beam deflections. In the subsequent section we extend our discussion to describe how to retain the sign information of the optical activity and hence how to determine the handedness of the optically active medium in a weak measurement. Although the weak scheme was initially proposed for quantum measurements [1], the same principle can be understood using a classical treatment [2, 3, 14, 15], as is the case here.

A light beam is assumed to propagate along the  $z'$  direction and is taken to be linearly polarized along  $x'$  (Fig. 1 and Fig. 2). Using Jones calculus the complex electric-field vector after

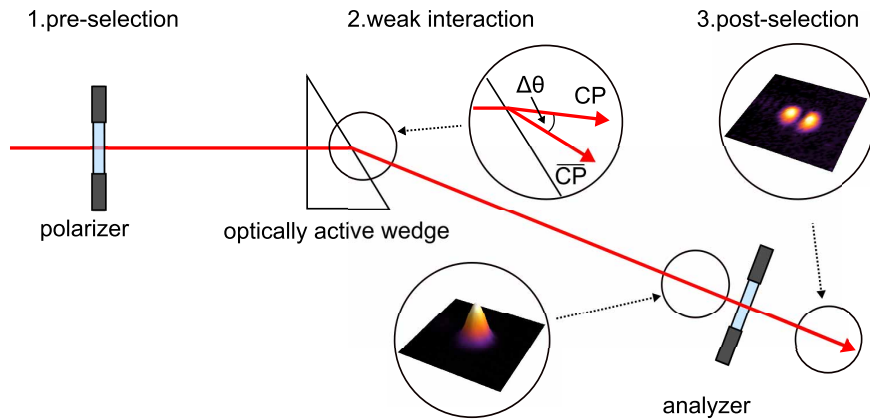


Fig. 1. Schematic of a weak measurement. It is based on three steps: (1) preparation of the system in a defined (polarization-) state (pre-selection), (2) weak interaction (perturbation) with the system giving rise to different angles of refraction for the two orthogonal circular polarization states ( $CP$ , and  $\bar{CP}$ ), and finally (3) post-selection of the final (polarization-) state.

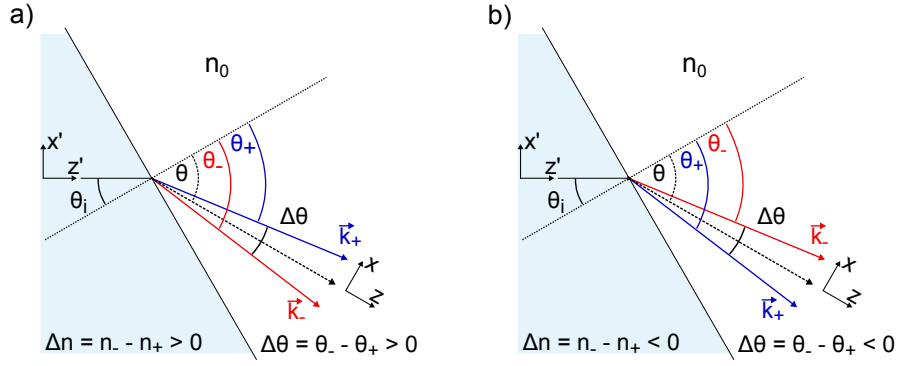


Fig. 2. Refraction geometry at a chiral-achiral interface for a positive (a) and negative (b) circular birefringence  $\Delta n$ .

the pre-selection polarizer is:

$$\mathbf{E}_1(x', y', z') = A_0(x', y') e^{ik_0 z'} |\hat{\mathbf{x}}'\rangle = \mathcal{E}_0 \exp\left[-\frac{x'^2 + y'^2}{w^2}\right] e^{ik_0 z'} \begin{pmatrix} 1 \\ 0 \end{pmatrix} \quad (1)$$

where  $w$  is the radius of the Gaussian beam and  $\mathbf{k}_0 \parallel \hat{\mathbf{z}}'$  the wavevector with  $|\mathbf{k}_0| = 2\pi n_0/\lambda$ . After refraction at the optically active prism surface the beam now propagates along  $z$  (Fig. 2). The weak interaction at the interface causes an angular deflection of the left- (−) and right- (+) circularly polarized beam components. Their angular beam separation is  $\Delta\theta = \theta_- - \theta_+$  (see Eq. (11)). For neat (undiluted) chiral liquids  $|\Delta\theta|$  is already  $\lesssim 10^{-6}$  rad and the beam separation even after  $\sim \text{m}$  is therefore always small ( $\sim \mu\text{m}$ ) compared to  $w$  ( $\sim \text{mm}$ ). A distance  $z_0$  after the interface the two Gaussian beam components are separated by  $2|\Delta x(z_0)|$  with  $\Delta x(z_0) = z_0 \tan(\Delta\theta/2)$ , so that one can write:

$$\mathbf{E}_2(x, y, z_0) = \frac{1}{\sqrt{2}} [A_- e^{i\mathbf{k}_- \cdot \mathbf{r}} |-\rangle + A_+ e^{i\mathbf{k}_+ \cdot \mathbf{r}} |+\rangle] \quad (2)$$

with

$$A_{\pm} = A_0(x \mp \Delta x(z_0), y) \quad \text{and} \quad \mathbf{k}_{\pm} = \frac{2\pi n_0}{\lambda} [\pm \sin(\Delta\theta/2) \hat{\mathbf{x}} + \cos(\Delta\theta/2) \hat{\mathbf{z}}],$$

where the refractive index of the surrounding medium is  $n_0$  (here air). The vectors  $|-\rangle$  and  $|+\rangle$  are respectively the normalized Jones vectors for the left- and right-circularly polarized components. Because the angular beam shift is so *weak*, the circular polarization components spatially overlap except for the outermost wings of the Gaussian beam. It follows that the center of the resulting beam is still linearly polarized, and only the edges contain circular polarization components. Post-selection is achieved with an analyzer set to an angle  $\beta_{pol}$  placed after the interface and in front of the detector. If  $\beta_{pol}$  is orthogonal to the initial polarization the center is extinguished and only the circular components at the wings of the Gaussian pass the analyzer. A weak value amplification takes place as the beam separation dramatically increases from a few  $\sim \text{nm}$  or less to the width of the light beam, typically  $\sim \text{mm}$ . This amplification is maximal for an orthogonal post-selection state [3]. However, the nature of the measurement has changed, as now the intensity becomes the measure of the weak interaction [2, 16]. The intensity after post-selection is directly proportional to the angular beam separation  $|\Delta\theta|$ . The bigger  $|\Delta\theta|$

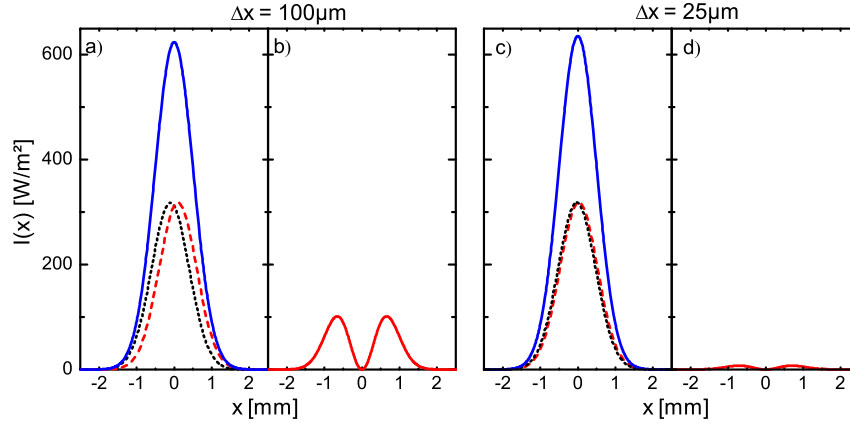


Fig. 3. Calculated intensities for the sum (solid blue line, a) and c)) of two separated and orthogonally polarized Gaussians (dashed lines, a) and c)) before and after post-selection (red line, (b) and (d)) for different beam displacements  $\Delta x$ . The amplitude of the post-selected intensity is directly proportional to  $|\Delta x|$  but not to the sign of  $\Delta x$ .

the more intensity passes the analyzer. This can be seen from the field vector and the expression for the intensity after the analyzer:

$$\begin{aligned} \mathbf{E}_3(x, y, z_0) &= \frac{1}{2} \left[ A_- e^{i(\mathbf{k}_- \cdot \mathbf{r} - \beta_{pol})} + A_+ e^{i(\mathbf{k}_+ \cdot \mathbf{r} + \beta_{pol})} \right] (\cos \beta_{pol} |\hat{\mathbf{x}}\rangle + \sin \beta_{pol} |\hat{\mathbf{y}}\rangle) \\ I_3(x, y, z_0) &= \frac{1}{2} c_0 \epsilon_0 |\mathbf{E}_3|^2 = \frac{c_0 \epsilon_0}{8} [A_+^2 + A_-^2 + 2 A_+ A_- \cos(\Delta \mathbf{k} \cdot \mathbf{r} + 2\beta_{pol})] \end{aligned} \quad (3)$$

where  $c_0$  and  $\epsilon_0$  are the speed of light and the permittivity of the vacuum, respectively. The difference between the two wavevectors  $\mathbf{k}_\pm$  corresponding to the separated circularly polarized modes is given by:

$$\Delta \mathbf{k} = \mathbf{k}_+ - \mathbf{k}_- = 2k_0 \sin \left[ \frac{\Delta \theta}{2} \right] \hat{\mathbf{x}} \quad (4)$$

Figure 3 shows plots of the intensities  $I_2(x, y, z_0)$  and  $I_3(x, y, z_0)$  calculated for two different beam displacements  $\Delta x(z_0)$  and an orthogonal post-selection polarizer (i.e.  $\beta_{pol} = 90^\circ$ ).  $I_2$  is a single Gaussian (Figs. 3a and 3c), while  $I_3$  shows two peaks separated by a distance comparable to the beam diameter (Figs. 3b and 3d). Here the peak intensity is proportional to the displacement of the beams. As can be seen from Fig. 3 and Eq. (3), the peak intensity after orthogonal post-selection is not sensitive to the sign of  $\Delta x(z_0)$ , i.e. the left- and right-circular components can not be distinguished when  $\beta_{pol} = 90^\circ$  as it is no longer clear which of the two polarization components deflects with  $\Delta x(z_0)$  and which one deflects with  $-\Delta x(z_0)$ . The sign information of the optical activity is consequently lost. Therefore it becomes necessary to combine weak value amplification with an appropriate polarization modulation scheme to retrieve the sign.

In optical activity measurements the linear polarization state will necessarily rotate as it traverses the optically active medium. However, the light beam traverses unequal distances through the optically active medium across the beam diameter, due to the necessary wedge geometry of the sample cell (Fig. 1), and so the optical rotation  $\alpha(x)$  also varies across the beam diameter. Eq. (3) has to be modified accordingly:

$$I'_3(x, y, z) = \frac{c_0 \epsilon_0}{8} \left\{ A_+^2 + A_-^2 + 2 A_+ A_- \cos \left[ 2 \left( k_0 \sin \left( \frac{\Delta \theta}{2} \right) x + \beta_{pol} - \alpha(x) \right) \right] \right\} \quad (5)$$



$$\beta_{FR}(t) = \Delta\beta \sin \omega_{FR} t,$$

the intensity  $I_3^{mod}(x, y, z_0, t)$  becomes time-dependent, which is illustrated in Fig. 5a. As can be seen from Eq. (7) the first term is constant and not of interest. The second term depends on the difference of the Gaussian amplitudes and is a measure of the splitting. It can be distinguished from the third term (product of Gaussians), since:

$$\begin{aligned} \sin[2\Delta\beta \sin \omega_{FR} t] &= 2J_1(2\Delta\beta) \sin \omega_{FR} t + \dots \\ \cos[2\Delta\beta \sin \omega_{FR} t] &= J_0(2\Delta\beta) + 2J_2(2\Delta\beta) \cos 2\omega_{FR} t + \dots \end{aligned} \quad (8)$$

Here  $J_0$ ,  $J_1$ , and  $J_2$  are the Bessel functions of the zeroth, first, and second order, respectively. It is seen that the second term is modulated at the fundamental,  $\omega_{FR}$ , whereas the third term depends on the harmonic  $2\omega_{FR}$ . Lock-in detection allows the second term and hence the beam separation to be discriminated from the third term, which is a function of the optical rotation  $\alpha(x)$ , via  $\Gamma(x)$ . Assuming that a position sensitive split detector is used for detection with  $I_3^{mod}$  centered on the two halves  $A$  and  $B$  of the photodetector, then the measured time-dependent power modulated at  $\omega_{FR}$  on each side of the detector can be calculated from:

$$P_{A, \omega_{FR}}(t) = \int_{-\infty}^{\infty} dy \int_{-\infty}^0 I_{3, \omega_{FR}}^{mod}(x, y, z_0, t) dx \quad \text{and} \quad P_{B, \omega_{FR}}(t) = \int_{-\infty}^{\infty} dy \int_0^{\infty} I_{3, \omega_{FR}}^{mod}(x, y, z_0, t) dx \quad (9)$$

The difference of the two signals is

$$\Delta P_{\omega_{FR}}(t) = P_{A, \omega_{FR}}(t) - P_{B, \omega_{FR}}(t) = P_0 J_1(2\Delta\beta) \operatorname{erf}\left[\frac{\sqrt{2} \Delta x(z_0)}{w}\right] \sin[\omega_{FR} t] \quad (10)$$

where  $P_0 = 0.25\pi\epsilon_0 c_0 \mathcal{E}_0^2 w^2$  is the power of the laser and  $\operatorname{erf}(x) = (2/\sqrt{\pi}) \int_0^x e^{-t^2} dt$  the error function. It is seen that the amplitude is proportional to  $|\Delta\theta|$  and the sign of the signal is proportional to the  $\operatorname{sgn}(\Delta\theta)$  (Fig. 5b). It follows that with this setup it is now possible to detect both the magnitude and the sign of the angular beam deflection  $\Delta\theta$ , whilst benefitting from the amplification offered by a weak value amplification scheme.

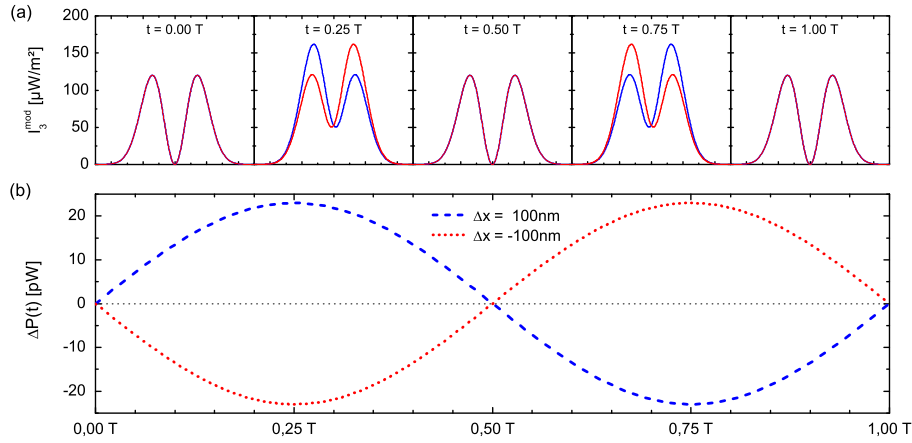


Fig. 5. (a) Intensity  $I_3^{mod}(x, y, z, t)$  at  $y = 0$  for beam displacements  $\Delta x = \pm 100 \text{ nm}$  calculated for different fractions of the period  $T$ . (b) Resulting time-dependent power difference  $\Delta P(t)$  calculated with Eq. (10) for  $\Delta x = \pm 100 \text{ nm}$ . Both signals have the same amplitude but are phase-shifted by  $\pi$ .



### 3. Measurements

#### 3.1. Experimental setup

For all the measurements presented here the setup is as shown in Fig. 4, where a position-sensitive dual anode-photomultiplier tube (Hamamatsu R5900U-04-M4) is used as a detector and placed at a fixed distance behind the sample prism. A Helium-Neon laser with  $\lambda = 633$  nm and an output power of  $P_0 \sim 7$  mW is taken as a light source. The (magneto-optical) Faraday effect in a glass prism serves as a model system for optical activity. The prism is made from SF11-glass ( $n=1.77$  and Verdet constant  $V = 14$  rad/Tm at  $\lambda = 633$  nm) and placed inside a longitudinal magnetic field induced by an electromagnet. The magnetic field strength is detected with a Gaussmeter (MAGSYS HGM09, resolution 0.1 Gauss, accuracy  $\pm 0.5\%$ ). The amplitude and the phase of  $\Delta P(t)$  are measured with a lock-in amplifier (LIA, Stanford Research Systems SR830).

The Faraday rotator consists of a 5 mm thick BK7 glass plate centered in a Helmholtz coil that is modulated at 187 Hz with an amplitude of  $\sim 100$  Gauss. This causes the plane of polarization of the light incident on the QWP to be rotated by  $\pm 5$  millidegree.

#### 3.2. Splitting of circular polarization beam components via the Faraday effect

Any isotropic medium becomes optically active and uniaxial in the presence of a longitudinal magnetic field (Faraday effect), and the angular divergence between the two refracted circular polarization components is [8, 13]

$$\Delta\theta \approx \frac{\Delta n \sin \theta_i}{n_0 \cos \theta} = \frac{VB \lambda \sin \theta_i}{\pi n_0 \cos \theta} \quad (11)$$

where  $\theta_i$  is the angle of incidence,  $\theta$  is the average of the two angles of refraction,  $\Delta n$  is the circular birefringence, and  $n_0$  is the refractive index of the surrounding medium. The angular

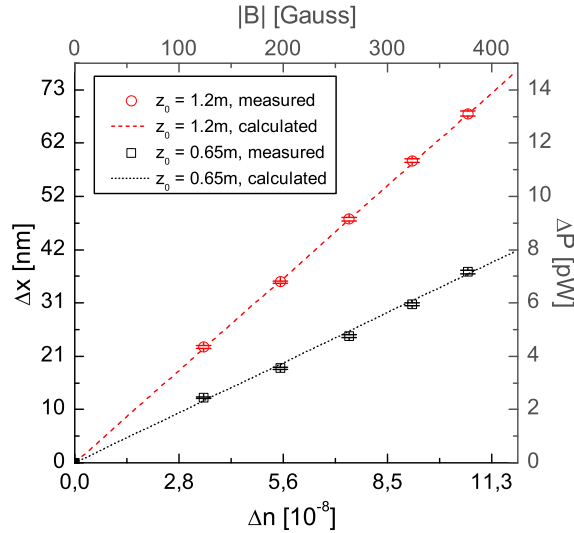


Fig. 6. Measurements of  $\Delta P$  for two different distances  $z_0$  between the prism surface and the post-selection analyzer P2 (see text for further details). The theoretically predicted power differences (Eq. (10)) are shown by the dashed lines.



divergence  $\Delta\theta$  is directly proportional to the magnetic optical activity, i.e. the magnetic field strength  $B$  and the Verdet constant  $V$  of the glass prism.

### 3.3. Angular measurement

First the optical activity is varied by changing the longitudinal magnetic field  $B$  across the glass prism, whilst detecting  $\Delta P(t)$ . Figure 6 shows the results for two measurements with the analyzer placed respectively at  $z_0 = 0.65$  m and  $z_0 = 1.2$  m after the prism. Each data point corresponds to an average over 100 measurements taken in 200 ms time intervals. It can be seen that as the distance between the interface and the post-selection polarizer increases, so does the intensity after the post-selection analyzer, in accordance with theory (dashed lines in Fig. 6). This is expected, as  $\Delta P$  is proportional to  $\Delta x(z_0) = z_0 \tan(\Delta\theta/2)$  (see Eq. (10)), and therefore scales linearly with distance. The distance  $z_0$  increases 1.846 fold in Fig. 6 and this is in good agreement with the experimentally observed increase in the slope of  $1.87 \pm 0.08$ . This clearly demonstrates that the setup is sensitive to the angular divergence  $\Delta\theta$ , as opposed to a lateral beam shift or some effect due to optical rotation.

### 3.4. Sign-recovery and sensitivity

To demonstrate that the measurements can be used to determine the absolute sign of the optical activity, we placed the post-selection polarizer P2 a distance  $z_0 = 1.2$  m after the prism and measured  $\Delta P(t)$  for opposite signs of the longitudinal magnetic field (optical activity). The results are depicted in Fig. 7a. Each data point is the average of 100 measurements taken in 200 ms time intervals. Both data sets match the theoretically predicted lines for  $\Delta P(t)$  (Eq. (10)). It follows that the sign (i.e. the direction) of the angular splitting, and hence the handedness are

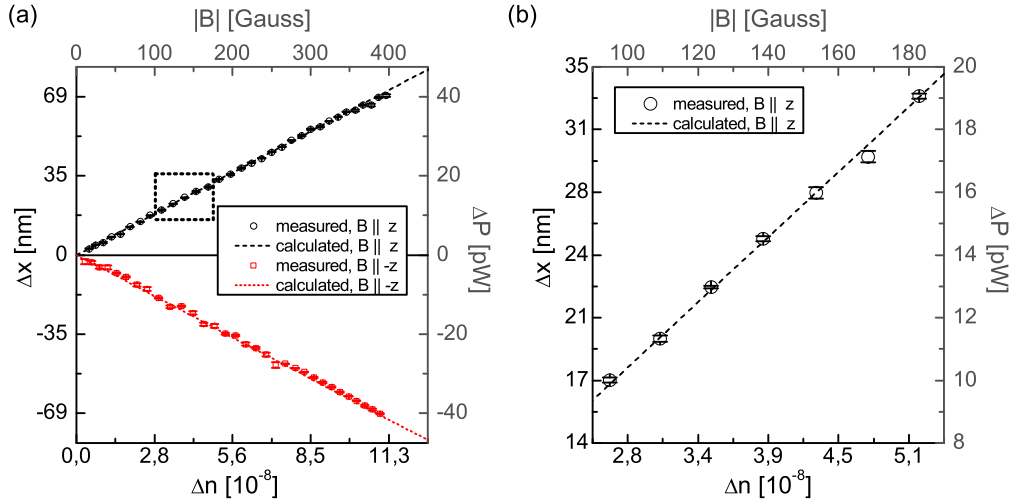


Fig. 7. (a) Measurement of  $\Delta P$  for  $d = 1.2$  m with  $\vec{B} \parallel \hat{z}$  (black) and  $\vec{B} \parallel -\hat{z}$  (red). Both data sets have the same magnitude but opposite sign. The measurements are in good agreement with theoretical predictions according Eq. (10) (dashed lines). (b) Zoom of a part of the measurement data in (a) marked by the box. The step size of  $\Delta B = 10$  Gauss corresponds to  $\Delta n = 3 \times 10^{-9}$  and  $\Delta\theta = 3$  nrad and is well resolved. In both diagrams  $\Delta x$  corresponds to the separation of the circular polarization components before the post-selection analyzer, and  $\Delta P$  is the intensity difference measured with the position sensitive detector after weak value amplification.

faithfully recovered in this weak value amplification scheme.

Figure 7b depicts a measurement of a region of Fig. 7a delineated by the box, where the optical activity is changed by smaller increments. It can be seen, that the data points are well separated, even though the magnetic field is only increased in 10 Gauss steps, which corresponds to a change in the circular birefringence of  $\Delta n = 3 \times 10^{-9}$ . This in turn corresponds to a change of  $\Delta\theta = 3$  nrad in the relative angle of refraction, which could be resolved with a relative error of  $s_{rel} \leq 1\%$ .

#### 4. Conclusions

We demonstrate a new form of optical activity measurement based on a modified weak value amplification scheme. Weak value amplification is a promising tool for detecting small polarization-dependent beam deflections, where the spatial beam separation is several orders of magnitude smaller than the beam diameter itself. Knowing in which direction the right- or the left-circular component refracted contains the information on the handedness of the optically active medium (e.g. the molecules' chirality). We have introduced a polarization modulation scheme, which makes it possible to determine the sign of the polarization-dependent beam splitting whilst still allowing for an amplification of up to  $\sim 10^6$  in the separation of the beam components compared with the actual separation (in the absence of weak value amplification). The modulation scheme is chosen so that it measures angular deflections and not optical rotation. We demonstrate that the scheme can be used to determine the absolute sign of the optical activity and to detect beam separations of  $\sim$  nanoradians with a relative error of  $s_{rel} \leq 1\%$ , which correspond to a circular birefringence of  $\Delta n \sim 1 \times 10^{-9}$ .

This sensitivity corresponds to an optical rotation  $\alpha = \pi\Delta n l/\lambda$  of about  $0.03^\circ$  in a polarimeter that uses a 10cm sample cell. However, unlike the polarimeter, which requires volumes of at least  $800\mu\text{l}$ , the refraction method requires a volume of less than  $4\mu\text{l}$ . An interesting prospect is to extend the present scheme by combining it with interferometric weak-value detection, where the resolution of  $\sim 1$  picorad in angular separation has been reported [5]. Such a sensitivity promises the analysis of  $0.00003^\circ$  solutions in  $\sim \mu\text{l}$  volumes, and would surpass the sensitivity of any commercial laboratory polarimeter.

#### Acknowledgments

This work was supported by an FhG internal program (Attract grant 692247).